Macrophages Shed Excess Cholesterol in Unique Extracellular Structures Containing Cholesterol Microdomains

Xueting Jin, Emilios K. Dimitriadis, Ying Liu, Christian A. Combs, Janet Chang, Neta Varsano, Erin Stempinski, Rhonda Flores, Shelley N. Jackson, Ludovic Muller, Amina S. Woods, Lia Addadi, Howard S. Kruth

Objective—Cells use various mechanisms to maintain cellular cholesterol homeostasis including efflux of cholesterol from the cellular plasma membrane to cholesterol acceptors such as HDLs (high-density lipoproteins). Little is known about the transfer of cholesterol from cells into the extracellular matrix. Using a unique monoclonal antibody that detects ordered cholesterol arrays (ie, cholesterol micro[or nano]-domains), we previously identified that particles containing these cholesterol domains accumulate in the extracellular matrix during cholesterol enrichment of human monocyte-derived macrophages and are found in atherosclerotic lesions. In this study, we further investigate these deposited particles containing cholesterol microdomains and discover their unexpected morphology.

Approach and Results—Although appearing spherical at the resolution of the conventional fluorescence microscope, super-resolution immunofluorescence and atomic force microscopy of in situ cholesterol microdomains, and immunoelectron microscopy of isolated cholesterol microdomains revealed that the microdomains are not vesicles or 3-dimensional crystals but rather appear as branching irregularly shaped deposits of varying size. These cholesterol microdomain-containing deposits are shed from the plasma membrane into the extracellular matrix.

Conclusions—To date, research on cellular excretion of excess cholesterol has demonstrated cellular cholesterol efflux in the form of membranous vesicles and discoidal HDL particles released into the fluid-phase medium. Shedding of plasma membrane cholesterol microdomains provides an additional mechanism for cells such as macrophages to maintain plasma membrane cholesterol homeostasis. Furthermore, recognition that macrophages shed cholesterol microdomains into the extracellular matrix is important to our understanding of extracellular buildup of cholesterol in atherosclerosis.

Visual Overview—An online visual overview is available for this article. **(*Arterioscler Thromb Vasc Biol*. 2018;38: 1504-1518. DOI: 10.1161/ATVBAHA.118.311269.)**

Key Words: atherosclerosis ■ cholesterol ■ fluorescence ■ homeostasis ■ macrophages

Plasma membrane cholesterol content and the formation of cholesterol microdomains affects the function of plasma membrane enzymes and receptors, ion transport, plasma membrane fluidity, and immune cell function.[1–5] Indeed, buildup of excess cholesterol within cellular membranes can be cytotoxic.[6,7] Thus, cells use multiple mechanisms to maintain cellular cholesterol homeostasis. To limit excess cholesterol accumulation, cells typically esterify cholesterol and store the esterified cholesterol in intracellular lipid droplets.[8] At the same time, cells traffic cholesterol to the plasma membrane for efflux to phospholipid-rich cholesterol acceptors such as plasma spherical HDL (high-density lipoprotein) particles synthesized by the liver and intestine.[9] In addition, cells can efflux cholesterol to nascent discoidal HDL that is synthesized by the cells themselves.[10] In this case, cellular ABCA1 (ATP-binding cassette transporter A1) mediates complexing of phospholipid with amphipathic apolipoproteins such as Apo (apolipoprotein) AI that circulate in the plasma or with ApoE synthesized by the effluxing cells.[10–14] Besides transfer of excess cellular cholesterol to HDL, in some cases, cholesterol-enriched cells release cholesterol into the surrounding medium within uni- and oligolamellar vesicular structures.[10,15–17]

See cover image

We have recently discovered that when macrophages accumulate large amounts of cholesterol during incubation with LDL (low-density lipoprotein), the macrophages not only store excess cholesterol within lipid droplets but also deposit excess unesterified cholesterol into the extracellular matrix both surrounding and underlying the macrophages.[18–22] We have used a unique

Received on: February 13, 2018; final version accepted on: May 16, 2018.

From the Experimental Atherosclerosis Section, National Heart, Lung, and Blood Institute (X.J., Y.L., J.C., R.F., H.S.K.), Scanning Probe Microscopy Unit, National Institute of Biomedical Imaging and Bioengineering (E.K.D.), Light Microscopy Core, National Heart, Lung, and Blood Institute (C.A.C.), Electron Microscopy Core, National Heart, Lung, and Blood Institute (E.S.), and Structural Biology Core, National Institute of Drug Abuse (S.N.J., L.M., A.S.W.), National Institutes of Health, Baltimore, MD; and Department of Structural Biology, Weizmann Institute of Science, Rehovot, Israel (N.V., L.A.).

The online-only Data Supplement is available with this article at http://atvb.ahajournals.org/lookup/suppl/doi:10.1161/ATVBAHA.118.311269/-/DC1.

Correspondence to Howard S. Kruth, MD, Experimental Atherosclerosis Section, National Heart, Lung, and Blood Institute, National Institutes of Health, Bldg 10, Room 5N-113, 10 Center Dr MSC 1422, Bethesda, MD 20892. E-mail kruthh@nhlbi.nih.gov

Nonstandard Abbreviations and Acronyms	
ABCA1	ATP-binding cassette transporter A1
ABCG1	ATP-binding cassette transporter G1
ACAT	acyl-coenzyme A: cholesterol acyltransferase
AcLDL	acetylated low-density lipoprotein
AFM	atomic force microscopy
Apo	apolipoprotein
BODIPY	4, 4-difluoro-4-borata-3a-azonia-4a-aza-s-indacene
DPBS	Dulbecco phosphate-buffered saline
FBS	fetal bovine serum
HDL	high-density lipoprotein
LDL	low-density lipoprotein
mAb	monoclonal antibody
M-CSF	macrophage-colony stimulating factor
SEM	scanning electron microscopy
STED	stimulated emission depletion
TO9	TO901317

anticholesterol microdomain monoclonal antibody (mAb) to detect this extracellular pool of cholesterol deposited by cultured cholesterol-enriched cells. The antibody (designated mAb 58B1) reacts with organized 2-dimensional 10 to 20 cholesterol molecule arrays hereafter referred to as cholesterol microdomains.[23] These cholesterol microdomains form when model phospholipid bilayer membranes are enriched with cholesterol.[24] Cholesterol-enrichment results in regions of lateral phase-separated pure cholesterol bilayers which are detected by mAb 58B1. MAb 58B1 does not react with monomeric cholesterol or esterified cholesterol; it does not react with LDL; and immunolabeling is lost after treatment of cholesterol microdomains with cholesterol oxidase.[23] The extracellular cholesterol microdomains not only occur in cultured cell systems but also accumulate within the extracellular matrix of atherosclerotic plaques.[18]

ABCA1 and ABCG1 (ATP-binding cassette transporter G1) are 2 ATP-binding cassette transporters involved in transport of intracellular cholesterol to the plasma membrane and efflux of cholesterol from cells.[9,25,26] Our earlier research has shown that both ABCA1 and ABCG1 mediate, in an additive manner, extracellular cholesterol microdomain deposition by cholesterol-enriched mouse M-CSF (macrophage colony-stimulating factor) differentiated bone marrow–derived macrophages, whereas ABCA1 alone mediates cholesterol microdomain deposition by cholesterol-enriched human M-CSF-differentiated monocyte-derived macrophages, the macrophage type used in the current study.[19,21] For both macrophage types, the liver X receptor agonist, TO9 (TO901317), increases deposition of cholesterol microdomains likely reflecting the known action of the liver X receptor transcription factor to upregulate ABCA1 and ABCG1 expression in cells.[19] Probucol is a drug that inhibits ABCA1-mediated functions including cholesterol transport to the plasma membrane.[27] Consistent with probucol inhibition of cholesterol transport to the plasma membrane, probucol completely blocks cholesterol microdomain deposition by human monocyte-derived macrophages but only partially inhibits cholesterol microdomain deposition by mouse bone marrow–derived macrophages because of the ABCG1 contribution to cholesterol microdomain deposition by this macrophage type.[21]

It is likely that cellular deposition of extracellular cholesterol microdomains is a means for cells to maintain cellular cholesterol homeostasis. Isolation of the extracellular cholesterol microdomains shows that their cholesterol content is almost completely unesterified.[22] Extracellular cholesterol microdomains can be mobilized by both plasma-derived and nascent HDL[18,19,22] and thus likely function in the so-called reverse cholesterol transport, the process by which peripheral cholesterol is returned to the liver for excretion into bile or reutilization depending on the body's overall cholesterol balance.

Because of the importance for cells to maintain cholesterol homeostasis and for excess cholesterol to be mobilized from peripheral tissues, where it can buildup and cause atherosclerosis, which can result in heart attacks and strokes, we undertook this study to learn more about the nature of the particles containing cholesterol microdomains deposited by macrophages into the extracellular matrix. Our findings show that cholesterol microdomains contained within unique branching irregularly shaped deposits are shed from the plasma membrane when cells are cholesterol enriched, a novel mechanism for the maintenance of plasma membrane cholesterol balance.

Materials and Methods

All data and supporting materials have been provided with the published article.

Materials

RPMI (Roswell Park Memorial Institute medium)-1640 was obtained from Mediatech (Herndon, VA); fetal bovine serum (FBS) and Dulbecco phosphate-buffered saline (DPBS) with Ca^{2+} and Mg^{2+} and without Ca^{2+} and Mg^{2+}, streptavidin-Alexa Fluor 488 and 594 conjugates, EDTA (ethylenediaminetetraacetic acid) solution (AM9260G), 0.25% trypsin-EDTA solution (25200056), 2.5% trypsin solution (15090046), and trypsin inhibitor solution (R-007-100) were all obtained from Invitrogen (Grand Island, NY); 6-well, 12-well, and 10-cm CellBIND culture plates and dishes were obtained from Corning (Corning, NY); T-75 CELLSTAR tissue culture flasks were obtained from Greiner Bio One (Monroe, NC); M-CSF and human interleukin-10 were obtained from PeproTech (Rocky Hill, NJ); AcLDL (acetylated low-density lipoprotein) and rabbit IgG anti-human LDL (J64398) were obtained from Alfa Aesar (Haverhill, MA); TO9 was obtained from Cayman Chemical (La Jolla, CA); penicillin-streptomycin, L-glutamine, filipin (F9765), poly-L-lysine (P1274), BSA (A7906), probucol (P9672), fatty acid-free BSA (A0281), cholesterol oxidase (C5421), Sandoz 58-035 (S9318), progesterone (P8783), and cholesterol (C3045) were obtained from Sigma (St. Louis, MO); mouse anticholesterol microdomain mAb 58B1 IgM in ascites was produced as previously described[28]; mouse anti-Clavibacter michiganense mAb (clone 9A1) IgM in ascites was obtained from Agdia (Elkhart, IN); paraformaldehyde, glutaraldehyde, and osmium tetroxide were obtained from Electron Microscopy Sciences (Hatfield, PA); biotinylated goat anti-mouse IgM and Vectashield hard set mounting medium without and with 4′,6-diamidino-2-phenylindole nuclear stain were obtained from Vector Laboratories (Burlingame, CA); ProLong Gold antifade mounting medium and Alexa Fluor 488–conjugated chicken anti-rabbit IgG (A21441) were from Thermo Fisher Scientific (Waltham, MA); BODIPY (4, 4-difluoro-4-borata-3a-azonia-4a-aza-s-indacene)-cholesterol linoleate was obtained from Setareh Biotech (Eugene, OR); goat anti-mouse IgM conjugated with 10-nm gold (ab39613) was from Abcam (Cambridge, MA); phosphotungstic acid was from Ted Pella (Reading, CA); rabbit IgG (SC-2027) was from Santa Cruz Biotechnology (Dallas, TX); FcR (fragment crystallizable region receptor) blocking reagent (130-059-901) was from Miltenyi Biotec (Auburn, CA); goat anti-ApoE (50A-G1a) and C1 (31A-G1a) were from Academy Bio-Medical (Houston,

TX); and male ApoE knockout C57BL/6J (002052) and wild-type (000664) control mice were obtained from the Jackson Laboratory (Bar Harbor, ME). Major Resources are given in Table in the online-only Data Supplement.

Culture of Human Monocyte-Derived Macrophages

Mononuclear cells were obtained from human donors by monocytopheresis, purified with counterflow centrifugal elutriation, and cultured as previously described.[29] Monocytapheresis was performed under a human subjects research protocol with informed consent approved by a National Institutes of Health institutional review board. The monocytes were centrifuged at 300*g* for 5 minutes at room temperature. Then, 25×10^6 monocytes were resuspended in 25 mL of complete medium (RPMI 1640 medium with 2 mmol/L L-glutamine, 50 ng/mL human M-CSF, 25 ng/mL interleukin-10, and 10% FBS) and seeded into a 75 cm^2 cell culture flask. Macrophage cultures were incubated in a 37°C cell culture incubator with 5% CO_2/95% air for 48 hours. Next, the cultures were rinsed 3× with 10 mL RPMI 1640 medium. After rinsing, fresh complete medium was added and medium was changed every 2 days until monocytes differentiated and proliferated sufficiently to become confluent. This required about 1 week of culture.

Experiments were initiated by rinsing the differentiated macrophages in the flask 3× with 10 mL DPBS without Ca^{2+} and Mg^{2+}, adding 10 mL 0.25% trypsin-EDTA solution, and incubating the flask at 37°C for 10 to 15 minutes to detach the macrophages. Next, 10 mL of RPMI 1640 medium containing 10% FBS was added to stop trypsinization. The macrophage cell suspension was centrifuged, resuspended in 1 mL of complete medium, counted, and seeded at desired densities in designated culture plates with complete medium. Macrophages were incubated 1 to 2 days before experiments were initiated with the indicated conditions. Human monocyte-derived macrophages were used for all experiments unless indicated otherwise.

Correlative Fluorescence and Scanning Electron Microscopy Analysis of Extracellular Cholesterol Microdomains

Ethanol-sterilized indium tin oxide coverslips with fiducial markers (CorrSlide, Optic Balzers, Lichtenstein) were coated at room temperature with a 0.1% (w/v) poly-L-lysine solution for 30 minutes. The coverslips were placed in a coverslip holder and rinsed in water by dipping, then dried on filter paper overnight.

For scanning electron microscopy (SEM) analysis, 2×10^5 macrophages were seeded onto the coverslips held within 6-well culture plates containing complete culture medium. After 2 days of incubation, the macrophages were rinsed 3× with RPMI 1640 and incubated 2 days with complete medium (without FBS) containing 50 µg/mL AcLDL and 5 µmol/L TO9. After incubation, macrophages were rinsed in DPBS and for SEM analysis without correlative fluorescence imaging, fixed in 2.5% (v/v) glutaraldehyde, 1% (v/v) paraformaldehyde, and 0.12 mol/L sodium cacodylate buffer, pH 7.3, for 1 hour at room temperature. Next, macrophages were postfixed with 1% (v/v) OsO_4 in the same buffer for 1 hour, dehydrated in an ethanol series, and critical point dried. The samples were then coated with 5 nm gold and imaged with a ZEISS Sigma HD VP scanning electron microscope (ZEISS, Jena Germany).

For correlative fluorescence and SEM analysis, cholesterol-enriched macrophages were immunostained at room temperature with anticholesterol microdomain mAb 58B1 as follows. Macrophages were rinsed 3× (5 minutes each rinse for this and all subsequent times) in DPBS, fixed for 10 minutes with 4% paraformaldehyde in DPBS, and rinsed an additional 3× in DPBS. Macrophages were then incubated 1 hour with 5 µg/mL purified mouse anticholesterol microdomain mAb 58B1 IgM diluted in DPBS containing 0.1% BSA. Control staining was performed with 5 µg/mL of an irrelevant purified mouse anti-Clavibacter michiganense mAb (clone 9A1) IgM diluted in DPBS containing 0.1% BSA. MAb IgM fractions were purified as previously described.[20] Macrophages were rinsed 3× in DPBS, followed by a 30-minute incubation in 5 µg/mL biotinylated goat anti-mouse IgM diluted in DPBS containing 0.1% BSA. After 3 rinses in DPBS, macrophages were incubated 10 minutes with 10 µg/mL streptavidin-Alexa Fluor 488 diluted in DPBS. Last, macrophages were rinsed 3× with DPBS, and fluorescence microscopic images of cholesterol microdomain fluorescence were obtained with a Zeiss LSM 780 microscope and C-apochromat 63×/1.20 water immersion objective using 488 nm wavelength for excitation and 490 to 552 nm wavelengths for fluorescence emission. After fluorescence imaging, macrophages were prepared for SEM analysis as described above including further fixation in glutaraldehyde and paraformaldehyde. SEM images of the same microscopic field were obtained using Zeiss Shuttle and Find software.

Because macrophages were not permeabilized, mAb 58B1 immunostaining represents cell surface and extracellular staining. No staining was observed when the control mAb was substituted for anticholesterol microdomain mAb 58B1 here and in subsequent procedures.

Specificity of mAb 58B1 for Cholesterol

Treatment of cholesterol-enriched macrophage cultures for 1.5 hour with cholesterol oxidase enzyme solution (0.16 U/mL DPBS) before mAb 58B1 immunostaining eliminated labeling of the extracellular cholesterol microdomains showing specificity of the Mab for cholesterol (Figure IB in the online-only Data Supplement). Treatment of the macrophage cultures with the same cholesterol oxidase solution in which cholesterol oxidase was inactivated by boiling 10 minutes showed preserved mAb 58B1 immunostaining of the cholesterol microdomains (Figure IA in the online-only Data Supplement).

Super-Resolution Stimulated Emission Depletion Fluorescence Microscopy Imaging of Cholesterol Microdomains

For fluorescence imaging by super-resolution stimulated emission depletion (STED) microscopy, 1×10^5 macrophages were cultured on poly-L-lysine–coated 12-mm diameter glass coverslips (0.16–0.19 mm thick) held within 12-well culture plates. Poly-L-lysine coating here and following was performed with 200 µg/mL in H_2O overnight at 37°C. After incubation for 2 days with 50 µg/mL AcLDL and 5 µmol/L TO9, macrophages were fixed and immunostained with the anticholesterol microdomain mAb 58B1 as described for conventional fluorescence microscopy above except that fluorescence labeling was performed with streptavidin-Alexa Fluor 594 conjugate. Macrophage coverslip cultures were mounted on glass microscope slides with ProLong Gold antifade mounting medium. Super-resolution microscopy was performed using the STED methodology. Time-gated STED images were obtained using a commercial STED microscope (SP8 STED 3X; Leica Microsystems, Wetzlar, Germany), equipped with a white-light laser and a pulsed 775-nm STED depletion laser. A 100×/1.4 numeric aperture oil immersion objective lens (HCX PL APO STED white; Leica Microsystems) was used for imaging. STED images were taken using 560-nm excitation, a scan speed of 600 lines per second, a 570- to 630-nm emission detection range with gated hybrid detectors, and the 775-nm STED depletion laser. The pixel size was 20 to 25 nm (1024×1024 pixels), and 6-line averages were performed.

Isolation of Extracellular Cholesterol Microdomains for Microscopic and Lipidomic Analysis

Macrophages obtained as described above were seeded into three 10-cm CellBind culture dishes (2×10^6 cells per dish). The macrophages were cultured 2 days in dishes with complete medium. Next, macrophages were rinsed 3× with RPMI-1640 medium before macrophages were incubated 2 days with RPMI-1640 medium alone, this medium containing 50 µg/mL AcLDL (to induce macrophage deposition of extracellular cholesterol microdomains) or AcLDL with 10 µmol/L probucol. For lipidomic analysis, macrophages were incubated 1 day with 135 µmol/L microcrystalline cholesterol prepared as described previously.[30] Microcrystalline cholesterol was used rather than AcLDL to avoid any contribution of lipids from AcLDL that

could be released from the culture surface along with the extracellular cholesterol microdomains.

No TO9 was included in these incubations because TO9 treatment made it difficult to release macrophages from the culture dish. Macrophages were removed from the culture dish by first incubating them for 30 minutes at 37°C in DPBS without Ca^{2+} and Mg^{2+} but containing 5 mmol/L EDTA. Then, the macrophages were detached with vigorous pipetting as needed. Next, the culture dishes were rinsed 3× with DPBS without Ca^{2+} and Mg^{2+}. This was followed by release of the cholesterol microdomains from the extracellular matrix using 2 mL of 2.5% trypsin solution per dish incubated for 30 minutes at 37°C. After incubation, the trypsin was neutralized by addition of 2 mL of trypsin inhibitor solution. The resulting cholesterol microdomain-containing solution was centrifuged in a polypropylene tube at 1000*g* for 2 minutes, and the supernatant containing the cholesterol microdomains was transferred to another polypropylene tube.

For isolation of cholesterol microdomains for microscopic analysis, the density of samples (1.5 mL) was adjusted to 1.21 g/mL using KBr (potassium bromide), and the density-adjusted sample was placed into a 2.5 mL ultracentrifuge tube (344625, Beckman, Indianapolis, IN). The tube was filled with density 1.21 g/mL KBr solution. Tubes were centrifuged 48 hours at 100 000*g* in an MLA-130 Beckman rotor to float the cholesterol microdomains, which were then obtained in the top 200 µL of sample removed from the centrifuge tube.

Cholesterol microdomains for lipidomic analysis were isolated by density gradient centrifugation as described previously[22] except that the cholesterol microdomain-containing supernatant from above was passed through a 0.45 µm syringe filter (Pall Corporation, PN4614) to remove any microcrystalline cholesterol before density gradient centrifugation. After density gradient centrifugation, fractions (*d*=1.04–1.05 g/mL) containing the cholesterol microdomains as determined by cholesterol analysis of the gradient as described previously[22] were pooled for lipidomic analysis described below.

Immunoelectron and Immunofluorescence Microscopy of Isolated Extracellular Cholesterol Microdomains

For immunofluorescence microscopy of isolated cholesterol microdomains, 20 µL of the cholesterol microdomain containing top fraction and control samples was placed onto glass slides. After the samples were air dried, the samples were immunolabeled with the anticholesterol microdomain antibody as described above for cultured macrophages prepared for correlative fluorescence microscopy and SEM. Samples were examined with an Olympus (Center Valley, PA) IX81 conventional fluorescence microscope and 40×/0.6 numeric aperture objective (LCP/PlanFl) using 480/40 nm excitation (40 refers to total bandwidth of the filter) and 535/50 nm emission filters.

For immunoelectron microscopy, 10 µL of sample diluted 20× with DPBS without Ca^{2+} and Mg^{2+} was placed onto a formvar-coated 200 mesh nickel grid stabilized with carbon (Ted Pella). All steps were performed at room temperature. After sample remained on the grid for 10 minutes to allow the cholesterol microdomains to adhere to the grid, sample fluid was removed with filter paper. Next, the grid was placed upside down on a 50-µL drop of DPBS without Ca^{2+} and Mg^{2+} containing 1% fatty acid-free BSA (all drops in succeeding steps were also 50 µL). After 30 minutes, the grid was transferred to a drop of DPBS without Ca^{2+} and Mg^{2+} containing 10 µg/mL anticholesterol microdomain mAb 58B1 and 0.1% fatty acid-free BSA. After 2 hours, the grids were rinsed by moving every 2 minutes between 5 drops of DPBS without Ca^{2+} and Mg^{2+} containing 0.1% fatty acid-free BSA. Then, grids were moved to a drop of DPBS without Ca^{2+} and Mg^{2+} containing 5 µg/mL of goat anti-mouse IgM conjugated with 10-nm gold particles. After 1 hour, grids were rinsed with 5 drops of DPBS without Ca^{2+} and Mg^{2+} followed by 5 drops of deionized H_2O and finally stained with 2% phosphotungstic acid. Samples were air dried and immediately examined with a JEOL (Peabody, MA) transmission electron microscope operated at 80 kV.

Lipidomic Analysis of Isolated Extracellular Cholesterol Microdomains

Total lipids were extracted from the sample (≈2 mL of fractions from density gradient centrifugation-isolated cholesterol microdomains) using a modified Folch extraction method.[31] Four milliliters of chloroform/methanol (2:1 v/v) was added to the sample. The sample was vortexed for 15 minutes. Then 1 mL of water was added, and the sample was vortexed for 1 minute. The mixture was centrifuged at 1100*g* for 15 minutes. The extraction results in an upper aqueous phase and a lower organic phase (containing lipids such as phospholipids, cerebrosides, and ceramides). The lower organic phase was evaporated to dryness using nitrogen, resuspended in 200 µL of chloroform and fractionated as follows. Classes of lipids were separated using 1 mL LC-NH2 (liquid chromatography-amino) solid-phase extraction tubes (SuperClean 50 mg bed weight; Sigma, St. Louis, MO) in a method similar to Bodennec et al.[32] The columns were first conditioned with 1 mL of hexane, and then 200 µL of the samples in chloroform was loaded onto the column. The fractions were retrieved using different solvents, and lipids contained in the resulting fractions are described in Table I in the online-only Data Supplement.

Next, samples were subjected to electrospray ionization mass spectrometric analysis using an Orbitrap Velos mass spectrometer (Thermo Fisher, San Jose, CA) with a static nanospray source with 4 µm spray tips and a capillary temperature of 200°C. The Fourier transform mass spectrometry mode with a mass resolution of 100 000 was used for all samples. All fractions were analyzed with a spray=1.5 kV, Rf (retardation factor)=60%, and 1 scan=1000 ms for the negative ion mode and 500 ms for the positive ion mode. Assignment of lipid species was based on accurate mass with mass error±1 ppm for the $[M\text{-}H_2O+H]^+$ mass peaks for cholesterol, $[M\text{-}H]^-$ mass peak for fatty acids, and the $[M+H]^+$ mass peaks for phosphatidylcholines and sphingomyelins. Tandem mass spectrometry analyses were also conducted to confirm the identification of the phosphatidylcholines and sphingomyelins species. Molar amounts for cholesterol, phosphatidylcholines, and sphingomyelins were determined from a calibration curve using a standard for each class of lipids.

Atomic Force Microscopy Imaging of Extracellular Cholesterol Microdomains

For atomic force microscopy (AFM) experiments, 1.6×10^5 macrophages per dish were seeded into poly-L-lysine–coated PELCO Clear Wall glass bottom dishes (14026-20, Ted Pella) containing 3 mL of complete medium per dish. Macrophages were incubated overnight before experiments were initiated with 1.5 mL of complete medium (without FBS) containing 50 µg/mL AcLDL and 5 µmol/L TO9. After a 2-day incubation, macrophages were rinsed, fixed, and immunostained for cholesterol microdomains with mAb 58B1 as described above.

Macrophages were imaged at room temperature and under DPBS buffer using an AFM instrument (Bioscope Catalyst AFM, Bruker-Nano, Santa Barbara, CA). The AFM sits atop an Olympus IX71 inverted microscope equipped with fluorescence and bright-field optics for simultaneous, colocalized observations. Imaging was performed with a 50×/0.5 numeric aperture Olympus objective (LMPlanFL) using 480/8 excitation and 535/50 emission filters. For AFM imaging, the AFM was operated in the Peak force tapping mode in which the probe is oscillated at frequencies far below resonance with the interaction force recorded at every cycle. The feedback keeps the peak force at each cycle constant, although the contact point of each force curve provides sample height information. In our experiments, we used soft, silicon nitride probes (MSCT, Bruker-Nano) whose stiffness was estimated by the thermal tune method. The peak force was kept at <500 piconewtons by the feedback, and we focused imaging to edges of macrophages and adjacent regions.

The mean height of the observed cholesterol microdomains was measured using the particle analysis module of the ImageJ software and custom-written code in Matlab (Mathworks, Inc, Natick, MA). In brief, microdomain populations were selected from AFM topography

images using ImageJ, and then each microdomain was thresholded at half-max height using the Matlab code. The corresponding area footprint and volume of each microdomain was then computed within the same Matlab code, and the mean microdomain height was calculated as the ratio of volume over area. The mean height data were then imported into Origin (OriginLab Corp, Northampton, MA), and histograms of microdomain height were constructed using appropriate bin sizes. Finally, the histograms were fitted within origin with Gaussian distribution functions to show the mean height of the shed microdomains and their size distribution.

Trafficking of Fluorescent BODIPY-Cholesterol

Macrophages (1×10^5) were seeded into 12-well CellBIND culture plates in complete medium. After incubation overnight, macrophages were incubated 1 day with 50 µg/mL AcLDL labeled with BODIPY-cholesterol linoleate (BODIPY is conjugated to cholesterol) and 5 µmol/L TO9 added to complete medium without FBS. Fluorescent BODIPY-cholesterol was used to learn whether this modified cholesterol molecule could traffic to extracellular cholesterol microdomains. BODIPY-cholesterol linoleate was incorporated into AcLDL at a ratio of 100 nmoles BODIPY-cholesterol linoleate to 1 mg AcLDL as described previously.[33]

After incubation with BODIPY-cholesterol linoleate-labeled AcLDL, macrophages were fixed and immunolabeled with the anticholesterol microdomain mAb 58B1 as described above for conventional fluorescence microscopy except that streptavidin-Alexa Fluor 594 was used in labeling of the cholesterol microdomains rather than streptavidin Alexa Fluor 488. Alexa Fluor 594–labeled cholesterol microdomain red fluorescence was imaged with an Olympus IX81 conventional fluorescence microscope using 560/55 nm excitation and 645/75 nm emission filters. BODIPY-cholesterol green fluorescence was imaged using 480/40 nm excitation and 535/50 nm emission filters.

Colocalization Analysis of Filipin Staining With Cholesterol Microdomains

Macrophages (2.5×10^6) were seeded per well into 6-well poly-L-lysine–coated CellBind culture plates and incubated overnight with complete medium. After incubation, macrophages were rinsed 3× with RPMI 1640 and incubated 2 days with complete medium (without FBS) containing 50 µg/mL AcLDL and 5 µmol/L TO9. After incubation, macrophages were rinsed, fixed, and immunostained with mAb 58B1 to label cholesterol microdomains as described above for conventional fluorescence microscopy. Next, macrophages were stained for 1 hour with filipin as previously described.[34] Macrophages were imaged in DPBS without a coverslip using an Olympus 20×/0.45 numeric aperture objective (LWD [long working distance] UPLAN FLUOR PH [fluorite phase]) and IX81 conventional fluorescence microscope. Filipin blue fluorescence was imaged using 350/50 nm excitation and 460/50 nm emission filters. Cholesterol microdomain green fluorescence was imaged using 480/40 nm excitation and 535/50 nm emission filters.

Detection of AcLDL Matrix Binding With Anti-LDL Immunostaining

AcLDL, either applied to a microscope slide and dried or after a 2-day incubation at a concentration of 50 µg/mL with macrophage cultures, was immunolabeled with an anti-LDL antibody that detects AcLDL. For incubated macrophages, the macrophages were removed from cultures as described above so that the extracellular matrix surrounding and underlying the macrophages could be immunolabeled. Then, in both cases, samples were rinsed 3× with DPBS and blocked 10 minutes at room temperature with FcR blocking reagent diluted 1:10 in DPBS. Next, samples were incubated with 10 µg/mL anti-LDL rabbit IgG in DPBS or control rabbit IgG, rinsed 3× with DPBS, incubated 30 minutes with 5 µg/mL Alexa Fluor 488–conjugated chicken anti-rabbit IgG in DPBS, rinsed 3× more with DPBS, and mounted with hard set mounting media containing 4′,6-diamidino-2-phenylindole.

Incubation of Macrophages With Agents That Affect Macrophage Cholesterol Metabolism

Differentiated human monocyte-derived and mouse bone marrow–derived macrophages were incubated 1 day with AcLDL (50 µg/mL)+TO9 (5 µmol/L) without or with the acyl-coenzyme A:cholesterol acyltransferase (ACAT) inhibitor, 58-035 (4 µg/mL). Bone marrow–derived mouse macrophages were obtained and cultured as described previously.[21] Human macrophages were incubated 1 day with AcLDL (50 µg/mL)+TO9 (5 µmol/L) with and without the cholesterol trafficking inhibitor, progesterone (10 µg/mL). After incubations, macrophages were rinsed with DPBS, fixed with paraformaldehyde, cholesterol microdomains were immunolabeled green with mAb 58B1, and nuclei were stained blue with 4′,6-diamidino-2-phenylindole that was incorporated into the mounting medium.

To assess the effect of ApoE deficiency on macrophage deposition of cholesterol microdomains, ApoE knockout and wild-type bone marrow–derived mouse macrophages were incubated 2 days with 50 µg/mL AcLDL+5 µmol/L TO9 to cholesterol-enrich macrophages and cause macrophage deposition of extracellular cholesterol microdomains. After incubations, cholesterol microdomains were immunolabeled as described above.

Immunocolocalization of ApoE and ApoC1 With Extracellular Cholesterol Microdomains

Differentiated human macrophages were seeded onto poly-L-lysine–coated glass coverslips and incubated overnight before a 2-day incubation with 50 µg/mL AcLDL+5 µmol/L TO9 to cholesterol-enrich macrophages and cause macrophage deposition of extracellular cholesterol microdomains. Then, macrophages were fixed at room temperature 10 minutes with 4% paraformaldehyde in DPBS before Fc (fragment crystallizable region) receptors were blocked with FcR-blocking reagent diluted 1:10 in DPBS containing 0.1% BSA. Next, macrophages were incubated overnight at 4°C with 5 µg/mL mouse mAb IgM 58B1 together with 1 µg/mL goat IgG polyclonal anti-ApoE or control goat IgG in DPBS containing 0.1% BSA. Primary antibodies were labeled 1 hour at room temperature with secondary antibodies using 5 µg/mL biotinylated rat anti-mouse IgM together with 2 µg/mL Alexa Fluor 488 (green) chicken anti-goat IgG in DPBS containing 0.1% BSA. Last, macrophages were incubated 10 minutes at room temperature with 10 µg/mL Alexa Fluor 594 (red) streptavidin to complete the immunolabeling of the cholesterol microdomains. Nuclei were stained blue with 4′,6-diamidino-2-phenylindole incorporated into the mounting medium. There were rinses with DPBS containing 0.1% BSA between all steps. Because there was no extracellular labeling of ApoC1 in a preliminary single apolipoprotein immunolabeling experiment, we did not carry out double immunolabeling for ApoC1 and cholesterol microdomains.

Results

SEM of Extracellular Cholesterol Microdomains

We performed SEM to examine at higher resolution the structure of the particles containing cholesterol microdomains that we reported previously.[18–22] Human monocyte-derived macrophages were incubated 2 days without or with 50 µg/mL AcLDL+5 µmol/L TO9 to enrich macrophages with cholesterol and to induce macrophage deposition of extracellular cholesterol microdomains. AcLDL is a modified LDL that is bound and endocytosed by macrophage scavenger receptors and thus, is an efficient way to cholesterol-enrich macrophages. After cholesterol enrichment, the macrophages were prepared for SEM using critical point drying. Macrophages that had been enriched with cholesterol showed numerous irregular and quasi-spherical shaped deposits attached to the

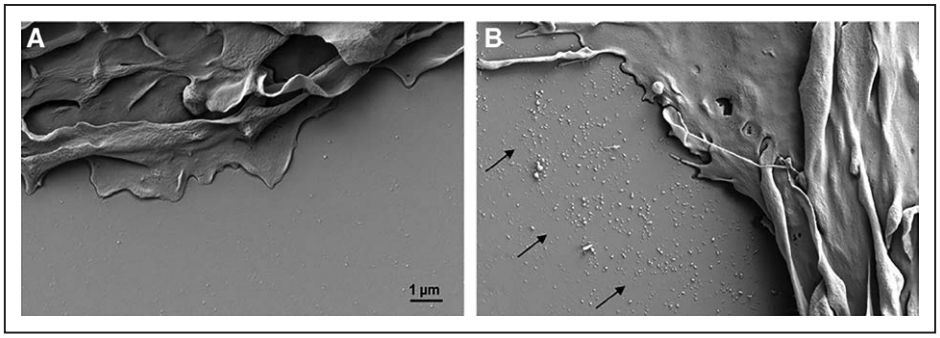

Figure 1. Scanning electron microscopy of macrophage extracellular particles deposited by cholesterol-enriched macrophages. Macrophages were incubated 2 days with 50 µg/mL AcLDL (acetylated low-density lipoprotein)+5 µmol/L TO9 (TO901317) to cholesterol-enrich macrophages and cause macrophage deposition of extracellular cholesterol microdomains. **A**, Almost no deposited particles surround macrophages that were not enriched with cholesterol by incubation with AcLDL. **B**, Many deposited particles (region indicated by arrows) surround macrophages that had been enriched with cholesterol.

culture surface that surrounded the macrophage plasma membrane (Figure 1B). The particles extended some 5 to 10 µm from the plasma membrane into the extracellular space. In contrast, there were only very sparse deposited material surrounding macrophages that had not been enriched with cholesterol (Figure 1A).

To determine whether any of the deposits detected by SEM were sites of cholesterol microdomains, we performed correlative fluorescence microscopy and SEM. In this procedure, cholesterol microdomains were first immunolabeled with the anticholesterol microdomain mAb 58B1, and conventional fluorescence microscopic images were obtained. Next, the cultured macrophages were prepared for SEM. Using fiducial markers, SEM images of the same macrophages were obtained. Figure 2 shows one such macrophage that had been enriched with cholesterol and, thus, had deposited extracellular cholesterol microdomains. Most but not all the deposits observed by SEM colocalized with cholesterol microdomains. Many of the smaller spherical particle deposits observed by SEM did not show cholesterol microdomains. These small spherical particles were likely AcLDL (the lipoprotein added to the culture to enrich the macrophages with cholesterol) that bound to the extracellular matrix. Immunostaining with an anti-LDL antibody showed that AcLDL also bound to the extracellular matrix surrounding the macrophages (Figure II in the online-only Data Supplement), but AcLDL itself did not label with anticholesterol microdomain mAb 58B1 (Figure III in the online-only Data Supplement).

STED Super-Resolution Fluorescence Microscopy of Extracellular and Plasma Membrane–Associated Cholesterol Microdomains

SEM indicated that the macrophage-deposited cholesterol microdomain-containing material was not perfectly spherical, although conventional fluorescence microscopy suggested otherwise. However, both conventional fluorescence microscopy and SEM techniques have limitations. The resolution of conventional fluorescence microscopy is about 200 nm. Thus, the true structure of objects below this size cannot be accurately determined by conventional fluorescence microscopy. On the other hand, structure as determined by SEM can be affected by the preparation of specimens for this type of analysis because specimens undergo critical point drying in which water is removed from the specimens by exposure to organic solvents. Organic solvents would be expected to remove varying degrees of lipid from the deposits. Thus, distortion of particle structure is likely with SEM.

Therefore, to examine the structure of the cholesterol microdomain-containing deposits at high microscopic

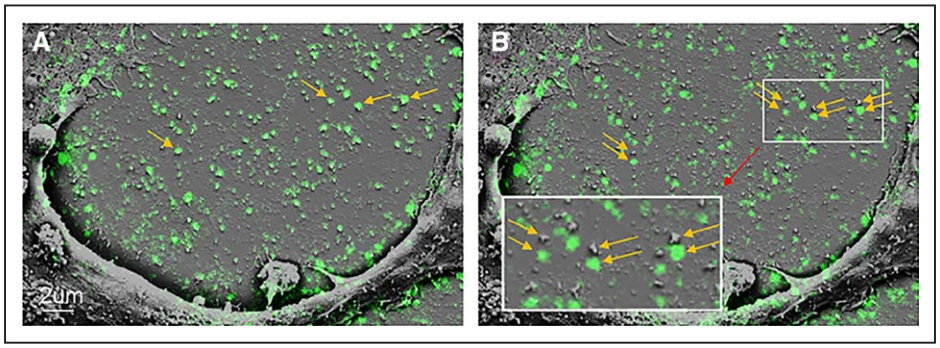

Figure 2. Correlative fluorescence and scanning electron microscopy (SEM) of macrophage-deposited cholesterol microdomains. Macrophages were incubated 2 days with 50 µg/mL AcLDL (acetylated low-density lipoprotein)+5 µmol/L TO9 (TO901317) to cholesterol-enrich macrophages and cause macrophage deposition of extracellular cholesterol microdomains. **A**, Superimposed fluorescence image of the green immunolabeled cholesterol microdomains with the corresponding SEM image of the same microscopic field. **B**, The fluorescence image is slightly offset below the corresponding SEM image to allow visualization of the underlying SEM structure of the cholesterol microdomains. Arrows indicate some of the particles containing cholesterol microdomains.

resolution but without exposure to organic solvents, we analyzed the cholesterol microdomains using STED fluorescence microscopy, a super-resolution fluorescence microscopy technique that allows resolution down to about 50 nm.[35] STED analysis revealed that the cholesterol microdomains were contained mostly in branching irregularly shaped structures of varying sizes (Figure 3A). These extracellular cholesterol microdomain-containing particles extended as much as 10 µm from the periphery of the plasma membrane, similar to what we observed by SEM.

Besides deposition of extracellular cholesterol microdomains, sometimes cholesterol microdomain-containing plasma membrane regions were also observed toward the top of the macrophages (Figure 3B; Figure IV in the online-only Data Supplement, a 3-dimensional confocal STED movie of the cholesterol microdomains). Quadrilateral regions (≤0.5 µm) that did not label with anticholesterol microdomain mAb 58B1 occurred within these plasma membrane cholesterol microdomain-containing areas of plasma membrane (Figure 3C).

AFM of Extracellular Cholesterol Microdomains

We confirmed the unexpected STED microscopic finding that cholesterol microdomains occurred in extracellular branching irregularly shaped structures with analysis using AFM, another high-resolution nondestructive imaging modality. AFM showed that control macrophages, which were not enriched with cholesterol (ie, were not incubated with AcLDL), exhibited a peripheral plasma membrane that was much less ruffled compared with macrophages that had been enriched with cholesterol (ie, incubated with AcLDL; compare Figure 4D, upper, and Figure 4D, lower). No significant extracellular deposits were observed on the culture surface next to control macrophages imaged by either mAb 58B1 immunolabeled cholesterol microdomains (Figure 4A and 4B, lower) or by AFM (Figure 4C and 4D, lower).

In contrast, the culture surface region adjacent to macrophages enriched with cholesterol was densely populated with deposits (Figure 4C and 4D, upper) corresponding to the cholesterol microdomains detected in the corresponding fluorescent image of mAb 58B1 immunolabeled cholesterol microdomains

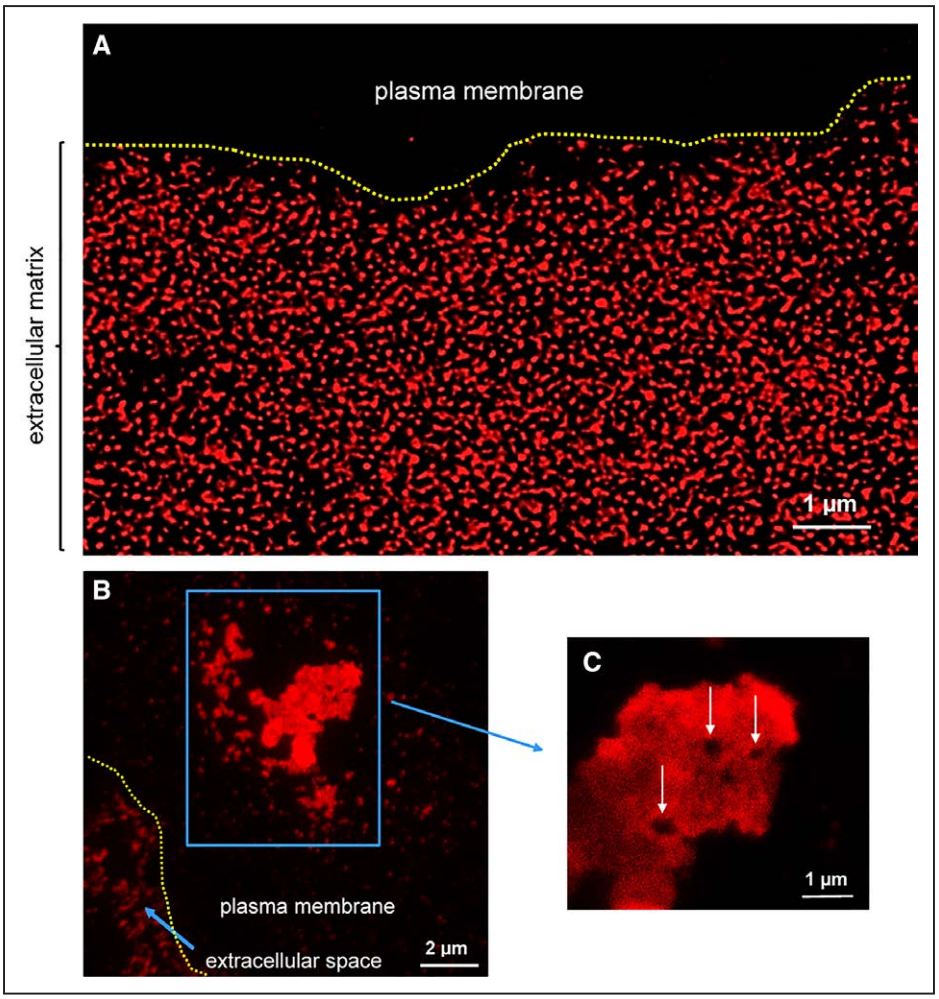

Figure 3. Super-resolution stimulated emission depletion (STED) fluorescence microscopy of cholesterol microdomains labeled with mAb 58B1. Macrophages were incubated 2 days with 50 µg/mL AcLDL (acetylated low-density lipoprotein)+5 µmol/L TO9 (TO901317) to cholesterol-enrich macrophages and cause macrophage generation of cholesterol microdomains. **A**, Extracellular immunolabeled cholesterol microdomains surrounding a macrophage. **B**, Cholesterol microdomains associated with the plasma membrane at the top of the macrophage (blue box), and within the extracellular space (short blue arrow). **C**, Note the quadrilateral voids (white arrows) occurring within the plasma membrane–associated cholesterol microdomains. Yellow-dotted line indicates plasma membrane extracellular space border.

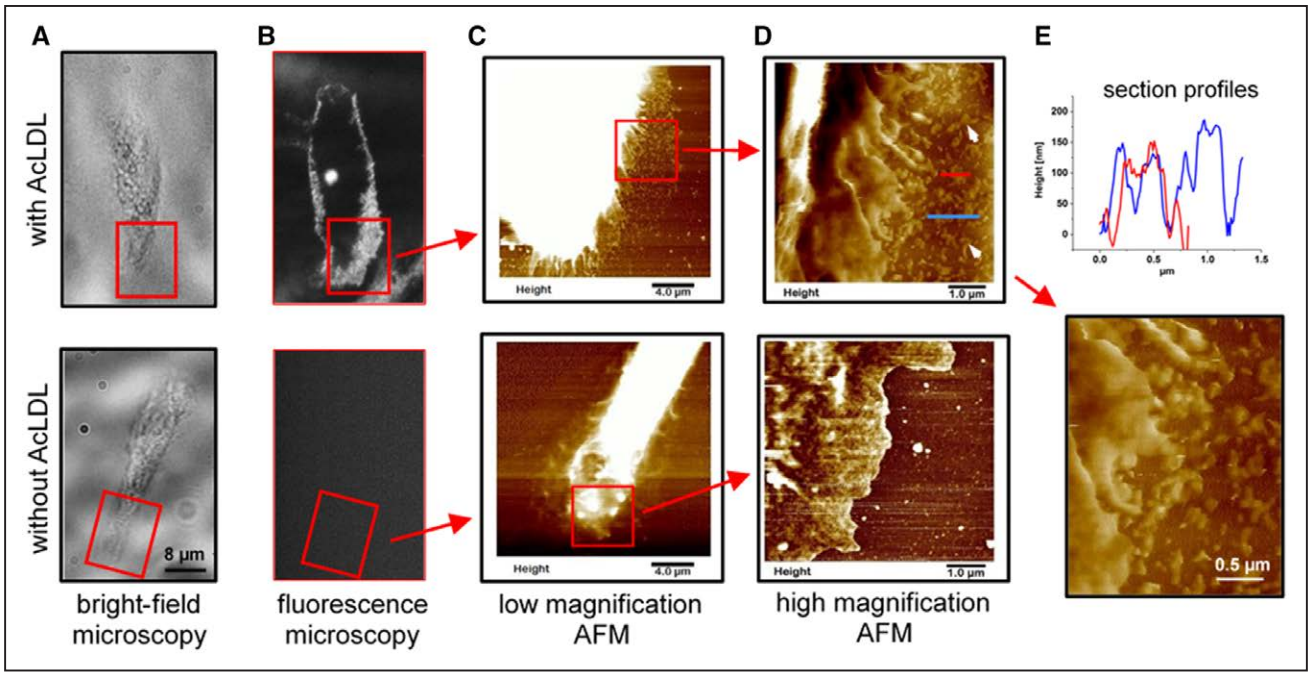

Figure 4. Atomic force microscopy (AFM) analysis of extracellular cholesterol microdomains. **A**–**D**, **Upper** (with AcLDL [acetylated low-density lipoprotein]) and **lower** (without AcLDL), Macrophages that were either cholesterol enriched by incubation with 50 µg/mL AcLDL+5 µmol/L TO9 (TO901317), or incubated without any addition for 2 days. **A**, Bright-field image, (**B**) corresponding fluorescence image of cholesterol microdomain immunolabeled macrophages, (**C**) low magnification AFM image of the boxed region in **A** and **B**, and (**D**) zoomed AFM image (11.7 nm/pixel) of the boxed region indicated in **C**. Red boxes in **A** and **B** show corresponding microscopic fields. In the AFM images, brighter regions are taller and the height scales for C were adjusted to make the plasma membrane and adjacent cholesterol microdomain deposits visible. The AFM image of cholesterol-enriched macrophage shows extensive plasma membrane ruffles and cholesterol microdomain deposits (arrows) adjacent to the macrophage (**D**, **upper**). **E**, **Upper**, Section height profiles along the lines running through the deposited cholesterol microdomains in **D**, **upper**. **E**, **Lower**, Deposited cholesterol microdomains at higher magnification. **A**–**D**, **Lower**, Corresponding images for a control cell that was not cholesterol enriched. The control macrophage lacks cholesterol microdomain immunolabeling (**B**, **lower**), shows less plasma membrane ruffling (**D**, **lower**), and lacks any deposited cholesterol microdomains (**D**, **lower**). Bar in **A**, lower, also applies to **A**, **upper**, image and both **B** images.

(Figure 4A and 4B, upper). These deposits were branching and irregularly shaped, and their lengths extended to as much as a few hundreds of nanometer, like characteristics of these deposits viewed by STED super-resolution fluorescence microscopy. The height above the culture surface of the deposits varied from cell to cell but for this macrophage ranged between 50 and 200 nm with the majority at the lower end of this scale (Figure 4E, upper; Figure V in the online-only Data Supplement). Examination of the ruffled edges of cholesterol-enriched macrophages showed some of the extracellular structures appeared to be in the process of shedding from the peripheral plasma membrane (Figure 4E, lower). Note that the extracellular deposits were not visible in bright-field images (Figure 4A, upper) but could only be visualized after fluorescence immunolabeling with mAb 58B1 (Figure 4B, upper) or with AFM as shown in Figure 4D, upper.

Some of the cholesterol microdomains that surrounded macrophages were deposited in a linear fashion extending out from the macrophage edge. Figure V, lower, in the online-only Data Supplement shows the AFM image and height distribution of these cholesterol microdomains, which tended to have heights (ranging 10–100 nm) that were less than the cholesterol microdomains discussed above.

Microscopic Analysis of Isolated Extracellular Cholesterol Microdomains

Cultured macrophages were enriched with cholesterol by incubation with 50 µg/mL AcLDL for 2 days in the absence or presence of probucol (10 µmol/L). As we previously showed that probucol, through its inhibition of ABCA1, almost completely inhibits human macrophage deposition of extracellular cholesterol microdomains,[19] the addition of probucol served as a control. Macrophages incubated without AcLDL served as another control. Cholesterol microdomains were isolated by flotation at d<1.21 g/mL of trypsin-released extracellular cholesterol microdomains as described in the Methods. Anticholesterol microdomain mAb 58B1 fluorescence immunolabeling of the floated lipid-containing fraction showed that only macrophages enriched with cholesterol generated substantial cholesterol microdomains (Figure 5B). Both controls, macrophages not enriched with cholesterol and macrophages enriched with cholesterol in the presence of the ABCA1 inhibitor, probucol, showed no and much-reduced cholesterol microdomains, respectively (Figure 5A and 5C).

Immunoelectron microscopic analysis of the sample with cholesterol microdomains (ie, fraction shown in Figure 5B above) showed that this fraction contained irregular branching structures that labeled both with anticholesterol microdomain mAb 58B1 immunogold label and with the phosphotungstic acid contrasting agent (Figure 6, arrows). The fraction also contained negatively stained spherical particles (arrowheads) that did not show mAb 58B1 immunogold labeling and were similar in size (≈22 nm) to AcLDL. (Negative staining means that the particles do not stain, but the particles are visible

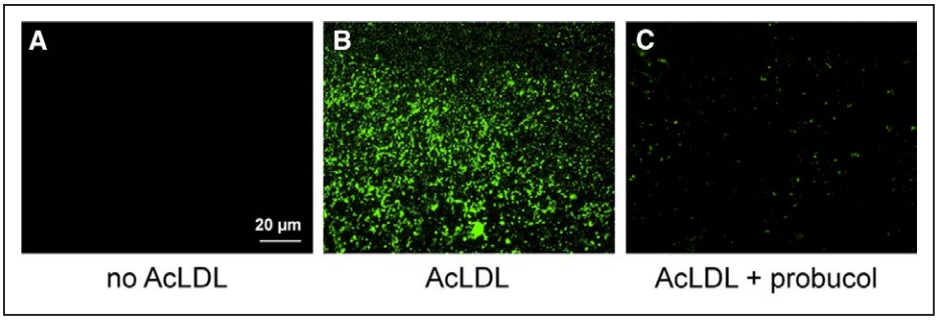

Figure 5. MAb 58B1 immunolabeling of isolated extracellular cholesterol microdomains. Macrophages were incubated 2 days with 50 µg/mL AcLDL (acetylated low-density lipoprotein) to cholesterol-enrich macrophages and cause macrophage deposition of extracellular cholesterol microdomains (**B**). Control macrophages were incubated without AcLDL (**A**) or with AcLDL and probucol (**C**) to inhibit deposition of cholesterol microdomains. Macrophages were removed from cultures with EDTA (ethylenediaminetetraacetic acid). Then, extracellular cholesterol microdomains were released from culture surfaces using trypsin, floated at d<1.21 g/mL, and immunolabeled with mAb 58B1 to reveal cholesterol microdomains. Only macrophages enriched with cholesterol deposited cholesterol microdomains (**B**), whereas no cholesterol microdomains were obtained from macrophages that were not cholesterol enriched (**A**). The ABCA1 (ATP-binding cassette transporter A1) inhibitor, probucol, substantially decreased generation of cholesterol microdomains by cholesterol-enriched macrophages (**C**).

because of the phosphotungstic acid stain that surrounds the particles.) As shown above (Figures II and III in the online-only Data Supplement), AcLDL was adherent to extracellular matrix, but AcLDL itself did not immunolabel with mAb 58B1. Thus, these small nonlabeled spherical particles were likely AcLDL that coisolated with the cholesterol microdomains. There was no immunogold labeling when the control irrelevant IgM antibody was substituted for anticholesterol microdomain mAb 58B1 IgM antibody.

Lipidomic Analysis of Isolated Extracellular Cholesterol Microdomains

Like that observed by incubating macrophages with AcLDL, macrophage enrichment with cholesterol by incubation with microcrystalline cholesterol induced deposition of extracellular cholesterol microdomains (Figure VI in the online-only Data Supplement), but avoided possible contamination by AcLDL of the isolated cholesterol microdomain phospholipids. Lipidomic analysis of the isolated cholesterol microdomains revealed that there were no lipid species detected in lipid extraction fractions 2, 4, and 6, which includes major lipid classes such as ceramides, cerebrosides, sulfatides, phosphatidylserines, and phosphatidylinositols (Table I in the online-only Data Supplement). Because of limited amount of material, we were not able to discriminate detected fatty acids from background levels. Cholesterol was detected in fraction 1 as $[M+H]^+$ and $[M-H_2O+H]^+$ mass peaks with the fragmented water loss peak being the larger of the 2 peaks. In fraction 5, 11 phosphatidylcholines and 2 sphingomyelins were detected as $[M+H]^+$ and $[M+Na]^+$ mass peaks with the protonated peak at least double the intensity of the sodiated peak (Table). The phosphatidylcholines/sphingomyelins molar ratio was about 9:1, whereas the cholesterol:phospholipid molar ratio was about 1:1.

Cholesterol Delivery to the Plasma Membrane Drives Deposition of Extracellular Cholesterol Microdomains

Shedding of cholesterol microdomains from the plasma membrane would be expected to depend on delivery of cholesterol to the plasma membrane. Previously, progesterone was shown to block delivery of AcLDL-derived cholesterol to the plasma membrane of macrophages after uptake and degradation of AcLDL.[36] Thus, we tested whether progesterone blocked macrophage plasma membrane shedding of cholesterol microdomains. This was the case (Figure 7).

One would expect that buildup of unesterified cholesterol within the macrophage should stimulate macrophage deposition of cholesterol microdomains. However, during incubation of macrophages with AcLDL, blocking macrophage

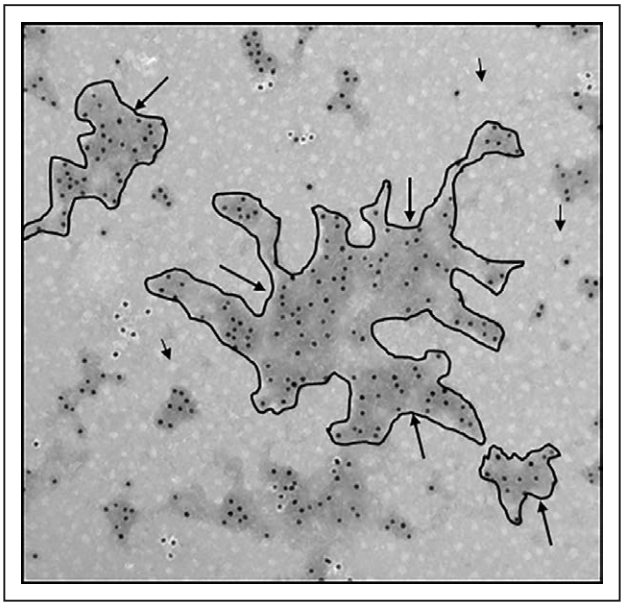

Figure 6. Immunoelectron microscopy showing mAb 58B1 gold-immunolabeled isolated cholesterol microdomains. Macrophages were incubated 2 days with 50 µg/mL AcLDL (acetylated low-density lipoprotein) to cholesterol-enrich macrophages and cause macrophage deposition of extracellular cholesterol microdomains. Macrophages were removed from cultures with EDTA (ethylenediaminetetraacetic acid). Then, extracellular cholesterol microdomains were released from culture surfaces using trypsin, floated at d<1.21 g/mL, and immunolabeled with mAb 58B1 followed by 10-nm gold-conjugated anti-mouse IgM antibody to show cholesterol microdomains. Some of the structures containing cholesterol microdomains are outlined in black and indicated by arrows. Note the great variation in shape and size of these structures. Short black arrows indicate AcLDL that coisolated with the cholesterol microdomains during their flotation. Ten-nanometers gold (black dots) serves as scale.

Table. Phospholipid Species in Isolated Extracellular Cholesterol Microdomains

Phospholipid Species	%
SM(d34:1)+H	7.0
SM(d34:0)+H	1.4
SM(d34:1)+Na	1.5
SM(d34:0)+Na	0.4
PC(32:1)+H	3.3
PC(32:0)+H	9.7
PC(32:1)+Na	0.3
PC(32:0)+Na	1.2
PC(34:2)+H	3.7
PC(34:1)+H	13.9
PC(34:2)+Na	1.6
PC 36a:4+H/PC34a:1+Na	16.5
PC(36:2)+H	5.8
PC(36:1)+H	5.5
PC(36:4)+Na	2.0
PC(38:5)+H/PC(36:2)+Na	7.0
PC(38:4)+H/PC(36:1)+Na	14.9
PC(38:5)+Na	1.4
PC(38:4)+Na	2.8

PC indicates phosphatidylcholine; and SM, sphingomyelin.

cholesterol esterification with the ACAT inhibitor, 58-035, did not increase human macrophage deposition of cholesterol microdomains (Figure VII in the online-only Data Supplement). We previously showed that the human M-CSF differentiated monocyte-derived macrophages used in this study accumulate large amounts of unesterified cholesterol during incubation with AcLDL even without addition of an ACAT inhibitor.[18,19] Thus, the lack of effect of addition of an ACAT inhibitor could have been because the amount of macrophage unesterified cholesterol was not rate limiting with respect to deposition of cholesterol microdomains.

On the other hand, mouse M-CSF differentiated bone marrow–derived macrophages do not show a large buildup of unesterified cholesterol during their incubation with AcLDL.[22] Thus, we examined whether addition of the ACAT inhibitor during incubation of these macrophages would stimulate cholesterol microdomain deposition by these macrophages. Figure VII in the online-only Data Supplement shows that macrophage cholesterol microdomain deposition was stimulated by ACAT inhibitor with these mouse macrophages.

ApoE mediates cholesterol efflux from macrophages,[12] and extracellular matrix and cell surface pools of ApoE have been demonstrated.[37] Thus, it was of interest to learn whether this apolipoprotein colocalized with the extracellular cholesterol microdomains. Double immunolabeling of deposited cholesterol microdomains and extracellular ApoE showed that, although ApoE was found associated with the macrophage cell surface and extracellular matrix, it did not colocalize with cholesterol microdomains (Figure VIII in the online-only Data Supplement). In addition, deficiency of ApoE in bone marrow–derived mouse macrophages did not affect macrophage deposition of extracellular cholesterol microdomains (Figure IX in the online-only Data Supplement). Another apolipoprotein expressed by macrophages, ApoC1,[38] also did not colocalize with cholesterol microdomains as it was not found in the extracellular matrix (data not shown).

BODIPY-Cholesterol Fails to Enter Extracellular Cholesterol Microdomains

Studies from the Ikonen laboratory have shown that fluorescent BODIPY-cholesterol linoleate incorporated into LDL can be used to trace the trafficking of LDL-derived cholesterol in cells.[33,39] LDL delivers BODIPY-cholesterol linoleate to cellular lysosomes where free BODIPY-cholesterol is generated after lysosomal hydrolytic release of linoleate from the BODIPY-cholesterol linoleate. Then, the free BODIPY-cholesterol traffics to the plasma membrane and endoplasmic reticulum, the latter where it is re-esterified and stored in lipid droplets. As previously observed for BODIPY-cholesterol linoleate incorporated into LDL,[33,39] we observed that for BODIPY-cholesterol linoleate incorporated into AcLDL, fluorescent BODIPY-cholesterol accumulated within intracellular inclusions known to include endosomal and lysosomal pools of cholesterol, and within the plasma membrane after a 24-hour incubation with this agent. Immunolabeling of these same macrophages with anticholesterol microdomain mAb 58B1 revealed that no BODIPY-cholesterol was present within the macrophage-deposited cholesterol microdomains (Figure 8).

Filipin Does Not Label Extracellular Cholesterol Microdomains

Filipin is a fluorescent polyene probe that labels molecular cholesterol within the plasma membrane and intracellular organelles such as lysosomes[34,40] and is commonly used in studies of cellular cholesterol metabolism. Therefore, it was of interest to learn whether this cholesterol-binding probe would also label the highly organized microdomain arrays of cholesterol that mAb 58B1 detects. Colocalization of filipin staining (blue) and mAb B58 immunolabeling (green) of cholesterol-enriched macrophages showed that although filipin uniformly labeled the plasma membrane, it did not label the extracellular cholesterol microdomains deposited by the macrophages (Figure X in the online-only Data Supplement).

Discussion

To date, research on cellular excretion of excess cholesterol has demonstrated cellular cholesterol release in the form of membranous vesicles and discoidal HDL particles released into the fluid-phase medium.[10,16] Some of the released membranous vesicles could be derived from exosomes,[17,41] the internal vesicles of multivesicular lysosomes that are released from cells when these lysosomes fuse with the plasma membrane. However, the macrophage-deposited extracellular cholesterol microdomains we characterize here are not exosomes as they are not vesicles (discussed below). Furthermore, exosomes are enriched with phosphatidylserine in an amount greater than sphingomyelin and ceramide in an amount greater than

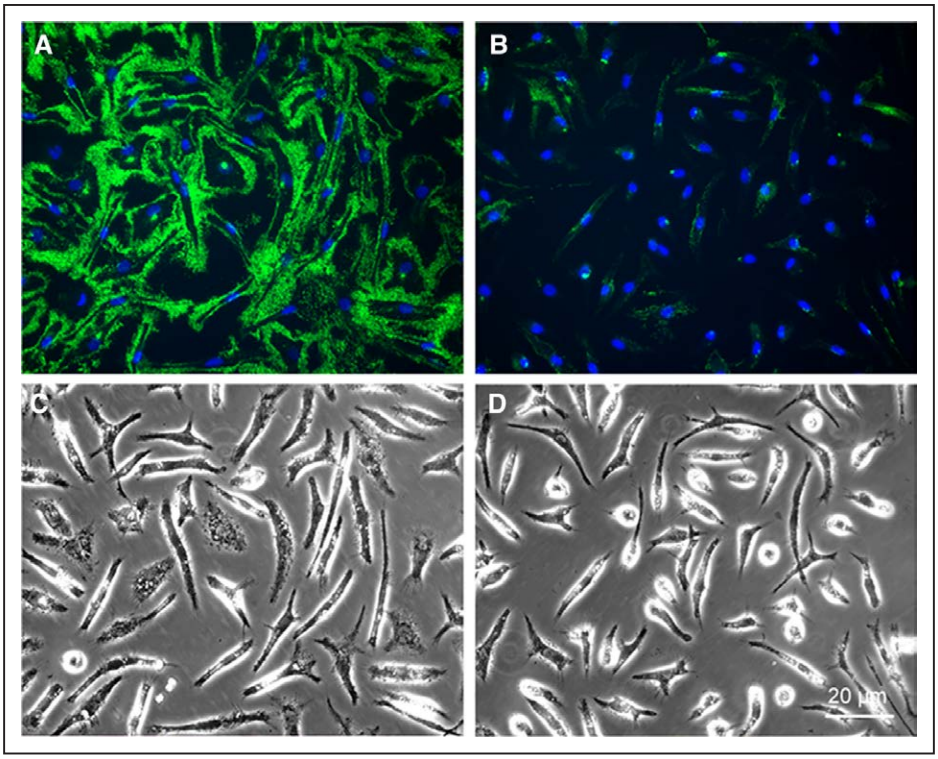

Figure 7. Progesterone inhibits macrophage deposition of extracellular cholesterol microdomains. Macrophages were incubated 1 day with 50 µg/mL AcLDL (acetylated low-density lipoprotein) and 5 µmol/L TO9 (TO901317) without (**A** and **C**) or with 10 µg/mL progesterone (**B** and **D**) to block cholesterol transport to the plasma membrane. After paraformaldehyde fixation, cholesterol microdomains were immunolabeled green with mAb 58B1 and nuclei were stained blue with 4′,6-diamidino-2-phenylindole (DAPI). **C**, **D**, Phase-microscopic images of their respective fluorescence images, **A** and **B**, above. Bar in **D** applies to all.

cholesterol.[42] This contrasts with the absence of ceramide or phosphatidylserine in the extracellular cholesterol microdomains. Besides their unique shape and cholesterol enrichment, in addition, our findings indicate the unexpected transfer process of shedding of the cholesterol microdomains from the plasma membrane into the extracellular matrix.

When viewed by conventional fluorescence microscopy, the extracellular cholesterol microdomains deposited by cholesterol-enriched human monocyte-derived macrophages appear spherical in shape. However, the findings of the current study reveal that the spherical shape was an artifact of the low resolution of conventional fluorescence microscopy.[41] Using STED super-resolution fluorescence microscopy, AFM of extracellular cholesterol microdomains in situ, and electron microscopy of isolated cholesterol microdomains, we have demonstrated that the structures containing cholesterol microdomains are not spherical but rather are branching irregularly shaped deposits. This finding of branching irregularly shaped cholesterol-containing structures was unexpected as previously observed biological structures enriched with cholesterol have usually shown needle- or plate-shaped crystals or membrane enveloped structures, the latter usually in the form of oligolamellar liposomes or spherical vesicles.[10,15,42,43] The structures containing the extracellular cholesterol microdomains did not show a crystalline, vesicular, or liposomal structure. Rather, our findings indicate that the cholesterol microdomains originate from cholesterol accumulation within the plasma membrane that then is shed into the extracellular matrix in the form of these branching irregularly shaped structures. Some of the shed extracellular cholesterol microdomains were arranged in a linear deposit extending from the macrophage edge suggesting that these deposits could have been derived from nanopodia, a type of thin cell extension associated with tetraspanin family cholesterol-binding proteins.[44] However, we did not detect any macrophage-associated tetraspanins with these deposits (X. Jin and H. Kruth, unpublished data).

The uniqueness of the mAb 58B1 that detects the cholesterol microdomains reported here should be emphasized in that this antibody does not label the plasma membrane unless there has been substantial cholesterol enrichment of cells. This contrasts with the commonly used cholesterol probe, filipin, that uniformly labels cellular plasma membranes. Filipin did not label the cholesterol microdomains, and thus, these cholesterol microdomains would not have been visualized in studies using filipin to study cholesterol trafficking. The lack of filipin staining of the cholesterol microdomains labeled by mAb 58B1 relates to the fact that filipin intersperses among mainly phosphatidylcholine molecules to bind molecularly dispersed cholesterol,[45] whereas filipin could not intersperse among the highly organized cholesterol structure in the microdomains.

We show here that buildup of unesterified cholesterol within macrophages promotes macrophage deposition of cholesterol microdomains. On the other hand, blocking the transport of this cholesterol to the plasma membrane with progesterone decreased macrophage deposition of cholesterol microdomains. Thus, cholesterol enrichment of the plasma membrane is closely linked with formation of cholesterol microdomains. This is consistent with our earlier findings that

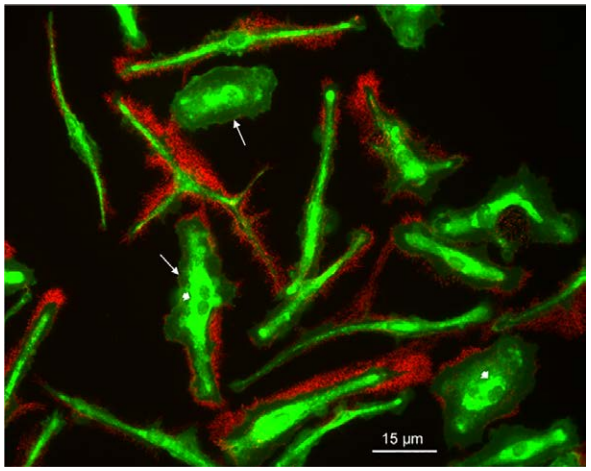

Figure 8. BODIPY (4, 4-difluoro-4-borata-3a-azonia-4a-aza-s-indacene)–labeled cholesterol does not deposit with extracellular cholesterol microdomains. Macrophages were incubated 1 day with 50 μg/mL AcLDL (acetylated low-density lipoprotein; with incorporated BODIPY-cholesterol linoleate) and 5 μmol/L TO9 (TO901317). Then, macrophages were fixed and immunolabeled with the anticholesterol microdomain mAb 58B1 indicated by red fluorescence. BODIPY-cholesterol is indicated by green fluorescence. Note that while BODIPY-cholesterol is present within the plasma membrane (arrows) and intracellular deposits (arrowheads), BODIPY-cholesterol does not enter extracellular cholesterol microdomains that surround the macrophages.

ABCA1 and ABCG1 proteins, known to mediate transport of excess cholesterol to the plasma membrane,[25,26] also mediate deposition of the extracellular cholesterol microdomains.[19,21]

In this regard, cholesterol enrichment of model cholesterol-phospholipid bilayers leads to the formation of lateral phase-separated cholesterol bilayer nanodomains (also referred to as 2-dimensional cholesterol crystals) within the phospholipid bilayers[46–50] (Figure 6 in Preston Mason et al[51]). The baseline cholesterol and phospholipid composition of the plasma membrane of human monocyte-derived macrophages is 25% cholesterol and 75% phospholipid.[52] Cholesterol enrichment of 40% to 54% of model supported phosphatidylcholine bilayer membranes induces cholesterol bilayer microdomains within the phosphatidylcholine bilayer membranes.[50,53] Similarly, in model phospholipid-cholesterol multilamellar liposomes, cholesterol bilayer microdomains begin to form at a cholesterol content >50%.[54] Cholesterol bilayer microdomains do not just occur in model bilayer membranes but also were shown in plasma membranes of smooth muscle cells isolated from rabbit atherosclerotic lesions.[47] These plasma membranes showed a 1/1 molar ratio of cholesterol/phospholipid consistent with the occurrence of cholesterol bilayer microdomains in model phospholipid-cholesterol bilayers at this ratio of cholesterol/phospholipid. The cholesterol microdomains isolated here showed a 1/1 molar ratio of cholesterol/phospholipid, and thus, the occurrence of cholesterol bilayer microdomains in these extracellular macrophage-deposited structures would be possible. The cholesterol microdomains we characterize here are not rafts, which are specialized cholesterol- and sphingomyelin-rich microdomains present within the plasma membrane. Lipidomic analysis of the isolated extracellular cholesterol microdomains showed that phosphatidylcholines outnumbered sphingomyelins about 9:1, and thus, the extracellular cholesterol microdomains are dissimilar to membrane rafts, which are enriched with sphingomyelins showing a phosphatidylcholines/sphingomyelins ratio of about 1:1.[52,55,56]

Cholesterol bilayer microdomains that form in model cholesterol-phospholipid bilayers show labeling with anti-cholesterol microdomain mAb 58B1,[24] and thus, cholesterol bilayer microdomains are the likely source of the extracellular mAb 58B1–labeled cholesterol microdomains that macrophages deposit into the extracellular matrix. Supporting this possibility is the finding that cholesterol enrichment of supported model phospholipid bilayer membranes induces elongated lipid protrusions emanating from the bilayer.[24,57,58] The released lipid protrusions spontaneously convert to spherical structures observed by conventional fluorescence microscopy (Figure 3A in Rahimi et al[58]). In a similar manner, cholesterol enrichment of macrophage plasma membranes could cause shedding of cholesterol bilayer microdomains that we observed with AFM.

Transfer of cholesterol microdomains from the plasma membrane into the extracellular matrix by the macrophages is also supported by our previous finding that treatment of macrophages with SU6656, a kinase inhibitor, causes accumulation of cholesterol microdomains on the plasma membrane rather than in the extracellular matrix.[18] The regular distribution of cholesterol microdomains underlying the macrophages and surrounding the macrophages could be because of transfer of the cholesterol microdomains into the extracellular matrix during contact of the plasma membrane with the extracellular matrix. The fact that cholesterol microdomains extend for a distance beyond the plasma membrane border most likely reflects that in the living state, the peripheral plasma membrane is very dynamic, showing membrane ruffling with extension and withdrawal of plasma membrane projections (Figure I in the online-only Data Supplement in Anzinger et al[59] for video showing motion of human M-CSF differentiated monocyte-derived macrophages like those used in this study). Like previous reports,[60,61] we observed that cholesterol enrichment of the macrophages increased plasma membrane ruffles, possibly promoting plasma membrane contact and transfer of plasma membrane cholesterol microdomains to the extracellular matrix.

Previously, we reported that the extracellular cholesterol microdomains did not show the plasma membrane marker CD14 and, thus, do not reflect random shedding of plasma membrane pieces.[22,62] The cholesterol microdomains are also shed very selectively from other pools of plasma membrane cholesterol. This was shown by the lack of shedding of plasma membrane BODIPY-cholesterol, derived from macrophage uptake of AcLDL carrying incorporated BODIPY-cholesterol linoleate. Although BODIPY-cholesterol did accumulate within intracellular inclusions and in the macrophage plasma membrane, it did not deposit within the extracellular matrix along with the cholesterol microdomains. This is consistent with the structural constraint imposed by the BODIPY fluorophore attached to the hydrophobic region of cholesterol that should prevent BODIPY-cholesterol from packing in an ordered tail-to-tail arrangement within the bilayer. Thus, BODIPY-cholesterol would not be expected to enter the

ordered cholesterol bilayer microdomains and, thus, would not be expected to be shed along with the ordered cholesterol bilayer microdomains, consistent with our findings. If cholesterol microdomains were released from macrophages by exocytosis of intracellular membranes, although BODIPY-cholesterol would not be incorporated into any released cholesterol microdomains, BODIPY-cholesterol present within noncholesterol microdomains should have deposited into the extracellular matrix and this was not the case.

MAb 58B1 also immunolabeled cholesterol microdomains regions that were present on the apical plasma membrane that likely does not contact the extracellular matrix. Interestingly, quadrilateral regions that did not immunolabel with mAb 58B1 occurred within these plasma membrane–associated cholesterol microdomains. The nonlabeled structures most likely were 3-dimensional cholesterol crystals similar to those occurring on the plasma membrane surface of cholesterol-enriched RAW 264 murine macrophages.[63] Three-dimensional cholesterol monohydrate crystals form in model phospholipid bilayer membranes when membranes are progressively enriched with cholesterol using cyclodextrin-cholesterol complexes to deliver cholesterol to the phospholipid bilayer or when mixtures of lipids and sufficient cholesterol are used to produce the bilayer membranes.[24,57,64] This occurs in phosphatidylcholine multilamellar liposomes when the cholesterol content is >66%.[64,65] The lack of mAb 58B1 immunolabeling of the crystalline structures formed within the plasma membrane–associated cholesterol microdomains is consistent with the observation that cholesterol monohydrate crystals do not immunolabel with mAb 58B1 on their large flat surface, but rather immunolabel only around their narrow edges.[28] We saw no microscopic evidence for the formation of cholesterol crystals in association with the macrophage-deposited extracellular cholesterol microdomains. Plasma membrane shedding of particles containing cholesterol microdomains could be a mechanism to prevent nucleation of cholesterol crystals by cholesterol bilayer microdomains at the plasma membrane surface where cholesterol is continuously being trafficked during cholesterol enrichment of cells.[66]

Macrophage-derived ApoE is an apolipoprotein that can mediate cholesterol efflux from human serum-differentiated macrophages that take up cholesterol crystals within surface-connected compartments by the process patocytosis.[67,68] Macrophage-derived ApoE localizes to these surface-connected compartments, which might facilitate ApoE mediation of cholesterol efflux from these macrophages. On the other hand, ApoE did not colocalize with the extracellular cholesterol microdomains, and ApoE absence did not affect the level of macrophage-deposited cholesterol microdomains. Previously, we showed that exogenously added ApoA1 (and ApoE in unpublished data) mediates mobilization of the extracellular cholesterol microdomains, most likely because of formation of nascent HDL, because mobilization depends on ABCA1.[18,22] Thus, one may have expected macrophage-derived ApoE to decrease cholesterol microdomains. However, it is likely that macrophage-derived ApoE concentration in the medium does not reach sufficient levels to mediate mobilization of the extracellular cholesterol microdomains.

Although in this report we have characterized the cholesterol microdomains deposited by cholesterol-enriched human monocyte-derived macrophages, we have also found that other cholesterol-enriched cells such as smooth muscle cells and endothelial cells also deposit extracellular cholesterol microdomains (unpublished data). This suggests that cells use extracellular deposition of cholesterol as a general mechanism to help maintain plasma membrane cholesterol homeostasis. This is significant because plasma membrane cholesterol content affects many cellular functions.[1–3] Furthermore, recognition that cells shed cholesterol microdomains is important to our understanding of diseases where cholesterol has been implicated in the pathogenesis of the disease such as atherosclerosis.

Acknowledgments

We thank the Department of Transfusion Medicine, Clinical Center, National Institutes of Health, for providing elutriated monocytes; Toshihiro Sakurai for guidance with the ultracentrifugal flotation; Dr Kirk Czymmek of Zeiss for help with analysis of correlative fluorescence and scanning electron microscopy data; Dr Xufeng Wu for help with correlative microscopy; National Institutes of Health Medical Arts and Daniela Malide for help with image processing.

Sources of Funding

This work was supported by the Intramural Research Program of the National Institutes of Health, and by the Binational Science Foundation (Grant 2013045). L. Addadi is the incumbent of the Dorothy and Patrick Gorman Professorial Chair of Biological Ultrastructure.

Disclosures

None.

References

1. Spector AA, Yorek MA. Membrane lipid composition and cellular function. *J Lipid Res*. 1985;26:1015–1035.
2. Bastiaanse EM, Höld KM, Van der Laarse A. The effect of membrane cholesterol content on ion transport processes in plasma membranes. *Cardiovasc Res*. 1997;33:272–283.
3. Subczynski WK, Pasenkiewicz-Gierula M, Widomska J, Mainali L, Raguz M. High cholesterol/low cholesterol: effects in biological membranes: a review. *Cell Biochem Biophys*. 2017;75:369–385. doi: 10.1007/s12013-017-0792-7.
4. Sorci-Thomas MG, Thomas MJ. Microdomains, inflammation, and atherosclerosis. *Circ Res*. 2016;118:679–691. doi: 10.1161/CIRCRESAHA.115.306246.
5. Kaul S, Xu H, Zabalawi M, Maruko E, Fulp BE, Bluemn T, Brzoza-Lewis KL, Gerelus M, Weerasekera R, Kallinger R, James R, Zhang YS, Thomas MJ, Sorci-Thomas MG. Lipid-free apolipoprotein A-I reduces progression of atherosclerosis by mobilizing microdomain cholesterol and attenuating the number of CD131 expressing cells: monitoring cholesterol homeostasis using the cellular ester to total cholesterol ratio. *J Am Heart Assoc*. 2016;5:e004401.
6. Kellner-Weibel G, Geng YJ, Rothblat GH. Cytotoxic cholesterol is generated by the hydrolysis of cytoplasmic cholesteryl ester and transported to the plasma membrane. *Atherosclerosis*. 1999;146:309–319.
7. Tabas I. Free cholesterol-induced cytotoxicity a possible contributing factor to macrophage foam cell necrosis in advanced atherosclerotic lesions. *Trends Cardiovasc Med*. 1997;7:256–263. doi: 10.1016/S1050-1738(97)00086-8.
8. Brown MS, Goldstein JL. Lipoprotein metabolism in the macrophage: implications for cholesterol deposition in atherosclerosis. *Annu Rev Biochem*. 1983;52:223–261. doi: 10.1146/annurev.bi.52.070183.001255.
9. Rosenson RS, Brewer HB Jr, Davidson WS, Fayad ZA, Fuster V, Goldstein J, Hellerstein M, Jiang XC, Phillips MC, Rader DJ, Remaley AT, Rothblat GH, Tall AR, Yvan-Charvet L. Cholesterol efflux and atheroprotection: advancing the concept of reverse cholesterol transport. *Circulation*. 2012;125:1905–1919. doi: 10.1161/CIRCULATIONAHA.111.066589.

10. Kruth HS, Skarlatos SI, Gaynor PM, Gamble W. Production of cholesterol-enriched nascent high density lipoproteins by human monocyte-derived macrophages is a mechanism that contributes to macrophage cholesterol efflux. *J Biol Chem*. 1994;269:24511–24518.
11. Basu SK, Ho YK, Brown MS, Bilheimer DW, Anderson RG, Goldstein JL. Biochemical and genetic studies of the apoprotein E secreted by mouse macrophages and human monocytes. *J Biol Chem*. 1982;257:9788–9795.
12. Zhang WY, Gaynor PM, Kruth HS. Apolipoprotein E produced by human monocyte-derived macrophages mediates cholesterol efflux that occurs in the absence of added cholesterol acceptors. *J Biol Chem*. 1996;271:28641–28646.
13. Wang S, Smith JD. ABCA1 and nascent HDL biogenesis. *Biofactors*. 2014;40:547–554. doi: 10.1002/biof.1187.
14. Gulshan K, Brubaker G, Conger H, Wang S, Zhang R, Hazen SL, Smith JD. PI(4,5)P2 is translocated by ABCA1 to the cell surface where it mediates apolipoprotein A1 binding and nascent HDL assembly. *Circ Res*. 2016;119:827–838. doi: 10.1161/CIRCRESAHA.116.308856.
15. Robenek H, Schmitz G. Ca++ antagonists and ACAT inhibitors promote cholesterol efflux from macrophages by different mechanisms. II. Characterization of intracellular morphologic changes. *Arteriosclerosis*. 1988;8:57–67.
16. Duong PT, Collins HL, Nickel M, Lund-Katz S, Rothblat GH, Phillips MC. Characterization of nascent HDL particles and microparticles formed by ABCA1-mediated efflux of cellular lipids to apoA-I. *J Lipid Res*. 2006;47:832–843. doi: 10.1194/jlr.M500531-JLR200.
17. Hafiane A, Genest J. ATP binding cassette A1 (ABCA1) mediates microparticle formation during high-density lipoprotein (HDL) biogenesis. *Atherosclerosis*. 2017;257:90–99. doi: 10.1016/j.atherosclerosis.2017.01.013.
18. Ong DS, Anzinger JJ, Leyva FJ, Rubin N, Addadi L, Kruth HS. Extracellular cholesterol-rich microdomains generated by human macrophages and their potential function in reverse cholesterol transport. *J Lipid Res*. 2010;51:2303–2313. doi: 10.1194/jlr.M005660.
19. Freeman SR, Jin X, Anzinger JJ, Xu Q, Purushothaman S, Fessler MB, Addadi L, Kruth HS. ABCG1-mediated generation of extracellular cholesterol microdomains. *J Lipid Res*. 2014;55:115–127. doi: 10.1194/jlr.M044552.
20. Kruth HS, Ifrim I, Chang J, Addadi L, Perl-Treves D, Zhang WY. Monoclonal antibody detection of plasma membrane cholesterol microdomains responsive to cholesterol trafficking. *J Lipid Res*. 2001;42:1492–1500.
21. Jin X, Freeman SR, Vaisman B, Liu Y, Chang J, Varsano N, Addadi L, Remaley A, Kruth HS. ABCA1 contributes to macrophage deposition of extracellular cholesterol. *J Lipid Res*. 2015;56:1720–1726. doi: 10.1194/jlr.M060053.
22. Jin X, Sviridov D, Liu Y, Vaisman B, Addadi L, Remaley AT, Kruth HS. ABCA1 (ATP-binding cassette transporter A1) mediates ApoA-I (Apolipoprotein A-I) and ApoA-I mimetic peptide mobilization of extracellular cholesterol microdomains deposited by macrophages. *Arterioscler Thromb Vasc Biol*. 2016;36:2283–2291. doi: 10.1161/ATVBAHA.116.308334.
23. Addadi L, Geva M, Kruth HS. Structural information about organized cholesterol domains from specific antibody recognition. *Biochim Biophys Acta*. 2003;1610:208–216.
24. Ziblat R, Fargion I, Leiserowitz L, Addadi L. Spontaneous formation of two-dimensional and three-dimensional cholesterol crystals in single hydrated lipid bilayers. *Biophys J*. 2012;103:255–264. doi: 10.1016/j.bpj.2012.05.025.
25. Vaughan AM, Oram JF. ABCA1 redistributes membrane cholesterol independent of apolipoprotein interactions. *J Lipid Res*. 2003;44:1373–1380. doi: 10.1194/jlr.M300078-JLR200.
26. Vaughan AM, Oram JF. ABCG1 redistributes cell cholesterol to domains removable by high density lipoprotein but not by lipid-depleted apolipoproteins. *J Biol Chem*. 2005;280:30150–30157. doi: 10.1074/jbc.M505368200.
27. Favari E, Zanotti I, Zimetti F, Ronda N, Bernini F, Rothblat GH. Probucol inhibits ABCA1-mediated cellular lipid efflux. *Arterioscler Thromb Vasc Biol*. 2004;24:2345–2350. doi: 10.1161/01.ATV.0000148706.15947.8a.
28. Perl-Treves D, Kessler N, Izhaky D, Addadi L. Monoclonal antibody recognition of cholesterol monohydrate crystal faces. *Chem Biol*. 1996;3:567–577.
29. Jin X, Kruth HS. Culture of macrophage colony-stimulating factor differentiated human monocyte-derived macrophages. *J Vis Exp*. 2016;112:e54244. doi: 10.3791/54244.
30. Skarlatos SI, Rouis M, Chapman MJ, Kruth HS. Heterogeneity of cellular cholesteryl ester accumulation by human monocyte-derived macrophages. *Atherosclerosis*. 1993;99:229–240.
31. Folch J, Lees M, Sloane Stanley GH. A simple method for the isolation and purification of total lipides from animal tissues. *J Biol Chem*. 1957;226:497–509.
32. Bodennec J, Koul O, Aguado I, Brichon G, Zwingelstein G, Portoukalian J. A procedure for fractionation of sphingolipid classes by solid-phase extraction on aminopropyl cartridges. *J Lipid Res*. 2000;41:1524–1531.
33. Kanerva K, Uronen RL, Blom T, Li S, Bittman R, Lappalainen P, Peränen J, Raposo G, Ikonen E. LDL cholesterol recycles to the plasma membrane via a Rab8a-Myosin5b-actin-dependent membrane transport route. *Dev Cell*. 2013;27:249–262. doi: 10.1016/j.devcel.2013.09.016.
34. Kruth HS, Comly ME, Butler JD, Vanier MT, Fink JK, Wenger DA, Patel S, Pentchev PG. Type C Niemann-Pick disease. Abnormal metabolism of low density lipoprotein in homozygous and heterozygous fibroblasts. *J Biol Chem*. 1986;261:16769–16774.
35. Hell SW, Wichmann J. Breaking the diffraction resolution limit by stimulated emission: stimulated-emission-depletion fluorescence microscopy. *Opt Lett*. 1994;19:780–782.
36. Mazzone T, Krishna M, Lange Y. Progesterone blocks intracellular translocation of free cholesterol derived from cholesteryl ester in macrophages. *J Lipid Res*. 1995;36:544–551.
37. Kockx M, Jessup W, Kritharides L. Regulation of endogenous apolipoprotein E secretion by macrophages. *Arterioscler Thromb Vasc Biol*. 2008;28:1060–1067. doi: 10.1161/ATVBAHA.108.164350.
38. Mak PA, Laffitte BA, Desrumaux C, Joseph SB, Curtiss LK, Mangelsdorf DJ, Tontonoz P, Edwards PA. Regulated expression of the apolipoprotein E/C-I/C-IV/C-II gene cluster in murine and human macrophages. A critical role for nuclear liver X receptors alpha and beta. *J Biol Chem*. 2002;277:31900–31908. doi: 10.1074/jbc.M202993200.
39. Hölttä-Vuori M, Sezgin E, Eggeling C, Ikonen E. Use of BODIPY-Cholesterol (TF-Chol) for visualizing lysosomal cholesterol accumulation. *Traffic*. 2016;17:1054–1057. doi: 10.1111/tra.12414.
40. Montesano R, Perrelet A, Vassalli P, Orci L. Absence of filipin-sterol complexes from large coated pits on the surface of culture cells. *Proc Natl Acad Sci USA*. 1979;76:6391–6395.
41. Blom H, Widengren J. Stimulated emission depletion microscopy. *Chem Rev*. 2017;117:7377–7427. doi: 10.1021/acs.chemrev.6b00653.
42. Chao FF, Amende LM, Blanchette-Mackie EJ, Skarlatos SI, Gamble W, Resau JH, Mergner WT, Kruth HS. Unesterified cholesterol-rich lipid particles in atherosclerotic lesions of human and rabbit aortas. *Am J Pathol*. 1988;131:73–83.
43. Kruth HS. Cholesterol deposition in atherosclerotic lesions. *Subcell Biochem*. 1997;28:319–362.
44. Zhang XA, Huang C. Tetraspanins and cell membrane tubular structures. *Cell Mol Life Sci*. 2012;69:2843–2852. doi: 10.1007/s00018-012-0954-0.
45. Milhaud J, Lancelin JM, Michels B, Blume A. Association of polyene antibiotics with sterol-free lipid membranes: I. Hydrophobic binding of filipin to dimyristoylphosphatidylcholine bilayers. *Biochim Biophys Acta*. 1996;1278:223–232.
46. Harris JS, Epps DE, Davio SR, Kézdy FJ. Evidence for transbilayer, tail-to-tail cholesterol dimers in dipalmitoylglycerophosphocholine liposomes. *Biochemistry*. 1995;34:3851–3857.
47. Tulenko TN, Chen M, Mason PE, Mason RP. Physical effects of cholesterol on arterial smooth muscle membranes: evidence of immiscible cholesterol domains and alterations in bilayer width during atherogenesis. *J Lipid Res*. 1998;39:947–956.
48. Ziblat R, Kjaer K, Leiserowitz L, Addadi L. Structure of cholesterol/lipid ordered domains in monolayers and single hydrated bilayers. *Angew Chem Int Ed Engl*. 2009;48:8958–8961.
49. Raguz M, Mainali L, Widomska J, Subczynski WK. The immiscible cholesterol bilayer domain exists as an integral part of phospholipid bilayer membranes. *Biochim Biophys Acta*. 2011;1808:1072–1080. doi: 10.1016/j.bbamem.2010.12.019.
50. Barrett MA, Zheng SB, Topponzi LA, Alsop RJ, Dies H, Wang A, Jago N, Moore M, Rheinstadter MC. Solubility of cholesterol in lipid membranes and the formation of immiscible cholesterol plaques at high cholesterol concentrations. *Soft Matter*. 2013;9:9342–9351.
51. Preston Mason R, Tulenko TN, Jacob RF. Direct evidence for cholesterol crystalline domains in biological membranes: role in human pathobiology. *Biochim Biophys Acta*. 2003;1610:198–207.
52. Gaus K, Rodriguez M, Ruberu KR, Gelissen I, Sloane TM, Kritharides L, Jessup W. Domain-specific lipid distribution in macrophage plasma membranes. *J Lipid Res*. 2005;46:1526–1538. doi: 10.1194/jlr.M500103-JLR200.
53. Ziblat R, Leiserowitz L, Addadi L. Crystalline domain structure and cholesterol crystal nucleation in single hydrated DPPC:cholesterol:POPC bilayers. *J Am Chem Soc*. 2010;132:9920–9927. doi: 10.1021/ja103975g.

54. Raguz M, Mainali L, Widomska J, Subczynski WK. Using spin-label electron paramagnetic resonance (EPR) to discriminate and characterize the cholesterol bilayer domain. *Chem Phys Lipids*. 2011;164:819–829. doi: 10.1016/j.chemphyslip.2011.08.001.
55. Brown DA, Rose JK. Sorting of GPI-anchored proteins to glycolipid-enriched membrane subdomains during transport to the apical cell surface. *Cell*. 1992;68:533–544.
56. Pike LJ, Han X, Chung KN, Gross RW. Lipid rafts are enriched in arachidonic acid and plasmenylethanolamine and their composition is independent of caveolin-1 expression: a quantitative electrospray ionization/mass spectrometric analysis. *Biochemistry*. 2002;41:2075–2088.
57. Varsano N, Fargion I, Wolf SG, Leiserowitz L, Addadi L. Formation of 3D cholesterol crystals from 2D nucleation sites in lipid bilayer membranes: implications for atherosclerosis. *J Am Chem Soc*. 2015;137:1601–1607. doi: 10.1021/ja511642t.
58. Rahimi M, Regan D, Arroyo M, Subramaniam AB, Stone HA, Staykova M. Shape transformations of lipid bilayers following rapid cholesterol uptake. *Biophys J*. 2016;111:2651–2657. doi: 10.1016/j.bpj.2016.11.016.
59. Anzinger JJ, Chang J, Xu Q, Buono C, Li Y, Leyva FJ, Park BC, Greene LE, Kruth HS. Native low-density lipoprotein uptake by macrophage colony-stimulating factor-differentiated human macrophages is mediated by macropinocytosis and micropinocytosis. *Arterioscler Thromb Vasc Biol*. 2010;30:2022–2031. doi: 10.1161/ATVBAHA.110.210849.
60. Adorni MP, Favari E, Ronda N, Granata A, Bellosta S, Arnaboldi L, Corsini A, Gatti R, Bernini F. Free cholesterol alters macrophage morphology and mobility by an ABCA1 dependent mechanism. *Atherosclerosis*. 2011;215:70–76. doi: 10.1016/j.atherosclerosis.2010.12.004.
61. Qin C, Nagao T, Grosheva I, Maxfield FR, Pierini LM. Elevated plasma membrane cholesterol content alters macrophage signaling and function. *Arterioscler Thromb Vasc Biol*. 2006;26:372–378. doi: 10.1161/01.ATV.0000197848.67999.e1.
62. Klotzsch E, Schütz GJ. A critical survey of methods to detect plasma membrane rafts. *Philos Trans R Soc Lond B Biol Sci*. 2013;368:20120033. doi: 10.1098/rstb.2012.0033.
63. Varsano N, Dadosh T, Kapishnikov S, Pereiro E, Shimoni E, Jin X, Kruth HS, Leiserowitz L, Addadi L. Development of correlative cryo-soft X-ray tomography and stochastic reconstruction microscopy. A study of cholesterol crystal early formation in cells. *J Am Chem Soc*. 2016;138:14931–14940. doi: 10.1021/jacs.6b07584.
64. Mainali L, Raguz M, Subczynski WK. Formation of cholesterol bilayer domains precedes formation of cholesterol crystals in cholesterol/dimyristoylphosphatidylcholine membranes: EPR and DSC studies. *J Phys Chem B*. 2013;117:8994–9003. doi: 10.1021/jp402394m.
65. Huang J, Buboltz JT, Feigenson GW. Maximum solubility of cholesterol in phosphatidylcholine and phosphatidylethanolamine bilayers. *Biochim Biophys Acta*. 1999;1417:89–100.
66. Infante RE, Radhakrishnan A. Continuous transport of a small fraction of plasma membrane cholesterol to endoplasmic reticulum regulates total cellular cholesterol. *Elife*. 2017;6:e25466.
67. Kruth HS, Skarlatos SI, Lilly K, Chang J, Ifrim I. Sequestration of acetylated LDL and cholesterol crystals by human monocyte-derived macrophages. *J Cell Biol*. 1995;129:133–145.
68. Kruth HS, Chang J, Ifrim I, Zhang WY. Characterization of patocytosis: endocytosis into macrophage surface-connected compartments. *Eur J Cell Biol*. 1999;78:91–99. doi: 10.1016/S0171-9335(99)80010-7.

Highlights

- Cholesterol-enriched macrophages deposit extracellularly cholesterol microdomains contained within unique branching irregularly shaped structures.
- The cholesterol microdomains are shed from the plasma membrane into the extracellular matrix when unesterified cholesterol increases in the macrophage and is transported to the plasma membrane.
- The lipid composition of shed cholesterol microdomains distinguishes them from plasma membrane rafts.
- Macrophage deposition of cholesterol microdomains helps explain buildup of cholesterol in the extracellular matrix of atherosclerotic lesions.